Eur. Phys. J. B **71**, 69–73 (2009)
DOI: 10.1140/epjb/e2009-00249-5

THE EUROPEAN PHYSICAL JOURNAL B

Regular Article

# Influence of disorder on the magnetism of graphene bilayers

Y.-X. Wang[a] and S.-J. Xiong

National Laboratory of Solid State Microstructures and Department of Physics, Nanjing University, 210093 Nanjing, P.R. China

Received 8 April 2009 / Received in final form 6 June 2009
Published online 15 July 2009 – 

**Abstract.** We numerically calculate the impact of site-energy disorder on the magnetism of biased bilayer graphene formed with the Bernal stacking. By using the mean-field method, we approximately solve the Hubbard Hamiltonian and calculate the average magnetization of the two layers, which indicates that the disorder does not change the nature of the first-order phase transition between paramagnetism and ferromagnetism, but may increase the critical interaction strength $U_c$ of the Hubbard Hamiltonian for the system to become the ferromagnetic phase. We also calculate the dependencies of relevant physical quantities on temperature. The implications of the results are discussed.

**PACS.** 73.22.-f Electronic structure of nanoscale materials: clusters, nanoparticles, nanotubes, and nanocrystals – 73.23.-b Electronic transport in mesoscopic systems – 75.30.-m Intrinsic properties of magnetically ordered materials

## 1 Introduction

Since graphene was successfully fabricated [1], in these years the system has been a hot topic and has triggered intensive researches both in theory and experiment due to its unusual electron characteristics of the linear dispersion relation near the two inequivalent points $\mathbf{K}$ and $\mathbf{K}'$ at the corners of the Brillouin zone [2]. Recently bilayer graphene (BLG) has also been made and shows almost equally exciting properties such as the parabolic dispersion relation at low energies and the Berry's phase of $2\pi$ [3]. A broad review about the properties of graphene has been given in reference [4].

The electron-electron (e-e) interactions are usually neglected in single layer graphene as they seem to play a minor role in the transport measurements [5,6]. However, when turn to the case of BLG, we can modulate the electron concentration of each layer by applying an external gate voltage. In this case, the electron-electron interaction may become an essential ingredient and needs further investigation. If the two layers are biased with opposite gate voltages, the system has nearly identical conduction and valence bands, and the interaction may drive electron-hole pair condensation between the layers [7].

The problem of e-e interactions become even more complex when combined with disorder. In the graphene systems, several works about disorder show that it is an indispensable factor in both the electron transport [8–12] and magnetism properties [13,14]. The disorder which preserves the chiral symmetry can reserve some delocalized states while those breaking this symmetry may lead to the Anderson localization of electron states.

The interaction in systems can cause abundant phenomena such as the counterflow superfluid behavior and the Kosterlitz-Thouless phase transition [15–17]. It was suggested that the Kosterlitz-Thouless critical temperature of the counterflow superfluid is reduced by introducing disorder [17]. It has recently been shown that when the long-range Coulomb interaction is replaced by the Hubbard on-site interaction, there will be a paramagnetic-ferromagnetic phase transition (PFPT) which is of the first-order and has a lower critical value of the on-site $U$ compared with the usual Stoner criterion [18].

Recent experimental investigation has revealed that a staggered potential which breaks the sublattice symmetry can be created in biased BLG [19,20]. As a result, an energy gap is opened at the Fermi energy which provides new possibilities of devising electronic components.

In this paper we investigate the effect of the site-energy disorder on the magnetism of biased BLG when the system is electron-doped compared with the half-filling. We use the mean-field approximation to deal with the Hubbard interaction. The results show that in comparison with the clean system the critical interaction in the Hubbard Hamiltonian increases as the site-energy disorder grows, but the first order nature of the PFPT is still retained.

## 2 Model and method

The system we consider consists of a BLG formed from two graphene layers with the Bernal stacking [21]. The

[a] e-mail: wangyixiang0406@gmail.com

two layers are coupled to opposite external gates. We can express the Hamiltonian of electrons in the biased disorder BLG system in terms of $\pi$ orbitals on carbon atoms. In the case of low carrier density the density of states (DOS) is large due to the band gap caused by the bias, the Coulomb interaction can be efficiently screened and we only need to consider the Hubbard on-site interaction:

$$H = H_{TB} + H_D + H_V + H_U, \tag{1}$$

where $H_{TB}$ is the tight-binding sub-Hamiltonian for the motion of single electrons in pure BLG, $H_D$, $H_V$ and $H_U$ are, respectively, the part of disordered site energies, the part of biased potential, and the on-site Hubbard interaction. These sub-Hamiltonians are explicitly written as:

$$H_{TB} = -t\sum_{l=1}^{2}\sum_{\vec{r},\sigma}\Big\{a^{\dagger}_{l,\sigma}(\vec{r})[b_{l,\sigma}(\vec{r}+\vec{a_1}) + b_{l,\sigma}(\vec{r}+\vec{a_2}) + b_{l,\sigma}(\vec{r}+\vec{a_3})] + h.c.\Big\} - t'\sum_{\vec{r},\sigma}\Big[a^{\dagger}_{1,\sigma}(\vec{r})b_{2\sigma}(\vec{r}) + h.c.\Big] \tag{2}$$

$$H_D = \sum_{l=1}^{2}\sum_{\vec{r},\sigma}\left[\epsilon^{a}_{l}(\vec{r})a^{\dagger}_{l,\sigma}(\vec{r})a_{l,\sigma}(\vec{r}) + \epsilon^{b}_{l}(\vec{r})b^{\dagger}_{l,\sigma}(\vec{r})b_{l,\sigma}(\vec{r})\right], \tag{3}$$

$$H_V = V\sum_{\vec{r},\sigma,s}\left[n_{1,s,\sigma}(\vec{r}) - n_{2,s,\sigma}(\vec{r})\right], \tag{4}$$

$$H_U = U\sum_{\vec{r},l,s} n_{l,s,\uparrow}(\vec{r})n_{l,s,\downarrow}(\vec{r}), \tag{5}$$

where $a_{l,\sigma}(\vec{r})$ ($b^{\dagger}_{l,\sigma}(\vec{r})$) is the annihilation operator for electron on site $A$ ($B$) of cell $\vec{r}$ in layer $l$ ($l = 1, 2$) with spin $\sigma$ ($\sigma = \uparrow, \downarrow$). $n_{l,s=a(b),\sigma}(\vec{r}) \equiv s^{\dagger}_{l,\sigma}(\vec{r})s_{l,\sigma}(\vec{r})$ is electron number operator. $\epsilon^{a(b)}_{l}(\vec{r})$ is the disorder induced site-energy on site $A$ ($B$) of cell $\vec{r}$ in layer $l$ which breaks the sublattice symmetry. We adopt a rectangular distribution probability, which is commonly used to study the generic case of Anderson localization [24],

$$P(\epsilon^{a,b}_{l}(\vec{r})) = \begin{cases} 1/g, & \text{for } -g/2 \le \epsilon^{a,b}_{l}(\vec{r}) \le g/2, \\ 0, & \text{otherwise,} \end{cases}$$

to characterize the strength of disorder. The basis vectors of the honeycomb lattice are $\vec{a_1} = (1, 0)a$ and $\vec{a_2} = (-\frac{1}{2}, \frac{\sqrt{3}}{2})a$ with $a = 2.46$ Å being the lattice constant, which define positions $\vec{r}$ of cells. $V$ is the applied bias potential which breaks the top-bottom symmetry of the system, and $U$ is the strength of the Hubbard on-site interaction. We take the in-plane nearest-neighbor (NN) hopping to be $t = 2.7$ eV [22] and the inter-plane NN hopping $t' = 0.39$ eV [23]. Below we will choose the bias voltage as $V = 0.08$ eV [20] which is assumed to be externally controlled. For the sake of simplicity we set $t$ as energy units in subsequent calculations.

As is well known, the Hubbard model in two-dimensions cannot be solved exactly without any approximation. By using the mean-field approach [18,25] in which all fluctuations at sites are frozen to deal with the Hubbard term, equation (5) can be rewritten as:

$$H_U = U\sum_{\vec{r},l,s,\sigma}\langle n_{l,s,\sigma}(\vec{r})\rangle n_{l,s,-\sigma}(\vec{r}) - U\sum_{\vec{r},l,s}\langle n_{l,s,\uparrow}(\vec{r})\rangle\langle n_{l,s,\downarrow}(\vec{r})\rangle, \tag{6}$$

where $\langle\ldots\rangle$ denotes the statistical averaging. The underlying idea of the mean-field method is that the dynamics at a given site can be considered as the interaction between the degrees of freedom on the site with an external bath created by all other degrees of freedom on other sites.

It is expected that there is an asymmetry between two layers for the charge density $n$ and magnetization $m = n_{\uparrow} - n_{\downarrow}$ due to the gate voltage [14,18]. Accordingly, we propose the following forms for the asymmetric spatial distributions in the ground state which also define the mean-field parameters: $\langle n_{1s\sigma}\rangle = \frac{2n+\Delta n}{4} + \sigma\frac{2m+\Delta m}{4}$ and $\langle n_{2s\sigma}\rangle = \frac{2n-\Delta n}{4} + \sigma\frac{2m-\Delta m}{4}$, where $n$ and $m$ are the average occupation number and magnetization on each site of the system, while $\Delta n$ and $\Delta m$ are the difference of the average occupation number and magnetization on each site between the two layers.

We take $10 \times 10$ sites for each layer and apply the periodical boundary condition in our numerical calculation. We investigate the magnetization of the system and the spatial distributions of charge and spin for systems deviating from the half filling in the presence of disorder. We choose the ferromagnetic state where all spins are aligned up as the initial trial wave function to carry out the self-consistent iteration. We perform configuration averaging over 100 random realizations.

## 3 Main results

At first, in Figure 1 we show the DOS (normalized to 1) of the biased BLG with different disorder strengths $g$ in the absence of interaction. We can see that there is a clear particle-hole symmetry, indicating that the site-energy disorder preserves this symmetry after configurational averaging. When $g = 0$, the DOS shows many spikes due to the finite-size effect. There are singularities of DOS at $E = \pm t$ and a large energy range at $E = 0$ with very low DOS due to the bias potential. When $g$ increases, the DOS at the Dirac point increases, while the singularities are smoothed away. Meanwhile, the width of the energy band increases with $g$. A more important point is that when there is no or low disorder, there is the high DOS at the edges of the band gap. But when the disorder strength increases, the gap which is due to the bias potential closes.

The behavior of DOS can be explained as follows. By introducing the disorder, lifetime of particle states with given momenta become no longer infinity. This is just a result of the scattering by the disorder. Thus, the Van-Hove

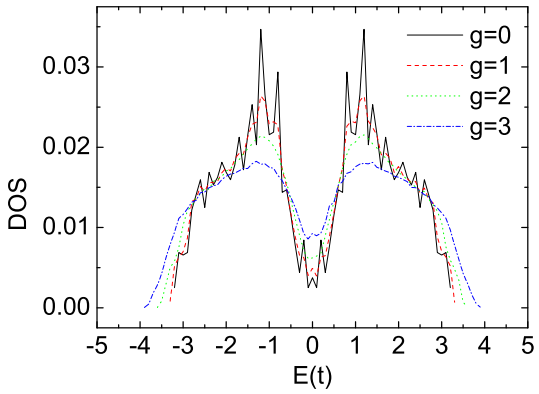


**Fig. 1.** (Color online) Density of states of bilayer graphene with different site-energy disorder strengths.

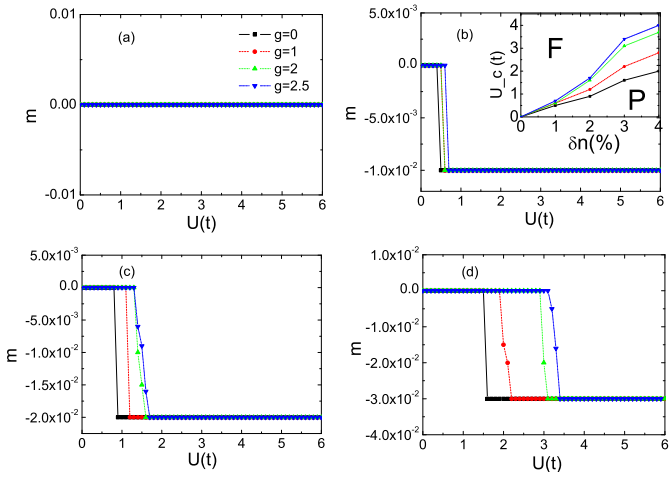


**Fig. 2.** (Color online) The average magnetization $m$ vs. the Hubbard strength $U$. (a), (b), (c), and (d) show the results in cases of doping densities $\delta n = 0\%, 1\%, 2\%$, and $3\%$, respectively. Different symbols correspond to different values of $g$, as indicated in (a). The inset in (b) shows the critical Hubbard strength $U_c$ vs. the doping density $\delta n$ for $g = 0$ and $g = 1$. F and P are the abbreviation of ferromagnetic and paramagnetic phase, respectively. The scale is the same as in (a).

singularities, which are related to particular momentum states in 2D and the onset of another energy band, are smeared out by the scattering. In other words, the accumulation of the states close to the position of the band edges of the pristine system is affected by the progressive raise of new states induced by disorder. Also the DOS shows a wider energy band reflecting the finite lifetime of the momentum states near the band edges. When the disorder strength increases to a larger value, the impact of disorder surpasses the effect of the bias potential and the gap disappears. Additionally, we can see that when the system is lightly doped and deviates from half filling, DOS at the Fermi level is not zero. This may enhance the screening of the long-range Coulomb interaction and support the assumption of on-site interaction in the Hubbard model.

Secondly, in Figure 2 we show that at the zero temperature $T = 0$, the relation between the average magnetization of each site $m$ and the doping density $\delta n$. We plot $m$ as a function of the Hubbard interaction strength $U$ for different values of $\delta n$ and disorder strength $g$. At half filling, for which there is average one electron at each site and $\delta n = 0$, from Figure 2a we can see that the average magnetization of the ground state is zero for all investigated values of $g$. Because the BLG system is a bipartite lattice and the site numbers in two sublattices are equal, this result is in accordance with the famous Lieb's theorem II which states that in the case of $U > 0$, for a bipartite lattice with a half-filled band the ground state has total spin $S = \frac{1}{2}||B| - |A||$, where $|A|(|B|)$ is the number of the sites in $A$ $(B)$ sublattice [26]. It is also shown that this behavior is robust against the site-energy disorder.

From Figures 2b–2d where the doping density is nonzero, we can see that if $U$ is small, the average magnetization of the ground state is zero. Further calculation shows that there exists no antiferromagnetic correlation, so the system is in the paramagnetic phase (PP). When $U$ grows and reaches a critical value, $U_c$, the system is changed to the ferromagnetic phase (FP) and $m$ increases to a finite value abruptly and then saturates by further increasing of $U$, indicating the system experiences a first-order phase transition [18]. This saturate value of the magnetization is equal to the full polarization of the doping charge, $m = \delta n$ [14,18] and is also robust against the change of site-energy disorder. However, the growing of the strength of disorder can cause the increase of the critical Hubbard interaction $U_c$ for the transition from PP to FP. This is the main conclusion of this paper.

In the inset of Figure 2b we show the phase diagram of PFPT and plot the dependence of the critical interaction strength $U_c$ on the doping density for different disorder strengths. It can be seen that the disorder evidently enhances $U_c$ for all investigated $\delta n$. $U_c$ increases almost linearly with the doping density and this behavior is more accurate at low doping densities.

The ferromagnetism is in fact induced by the combined effects of the on-site Hubbard interaction and the long-range correlation among local moments mediated by conduction electrons. It is known that the diagonal disorder can localize electrons in graphene and the extent of localization increases with the disorder strength [8,10]. So the disorder weakens the long-range ferromagnetic correlation due to the localization of conduction electrons. When the strength of disorder increases, the correlation between electrons decreases. To keep ferromagnetism, a larger critical $U_c$ is needed.

To explain our results better, we plot the spatial distributions of charge and spin with the doping density $\delta n = 1\%$ for PP $(U = 0.2)$ and FP $(U = 2)$ phases in Figures 3 and 4, respectively. In the charge distribution plot, we introduce the quantity $\Delta n(x, y) = n(x, y) - 1$, the difference between the charge occupation number and one at each site. It is shown that the site-energy disorder can cause large fluctuations of charge and spin distributions both in PP and FP. In PP the extra electrons prefer to stay in the bottom layer, as the potential is lower than

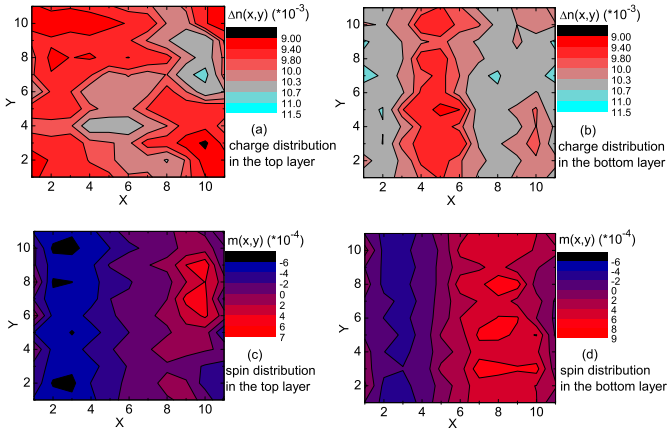


**Fig. 3.** (Color online) The charge and magnetization distributions in two layers for disorder strength $g = 1$ and interaction strength $U = 0.2$.

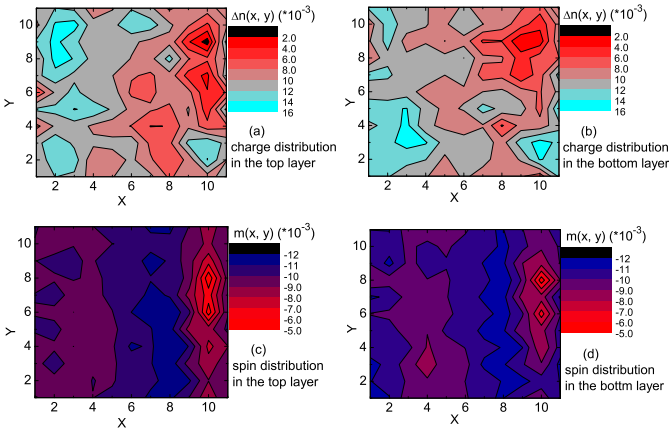


**Fig. 4.** (Color online) The charge and magnetization distributions in two layers for disorder strength $g = 1$ and interaction strength $U = 2$.

that in the top layer due to the gate voltage. However, in FP ($U = 2$), the doping electrons are evenly distributed in two layers because the effect of the interaction of the Hubbard interaction and disorder may surpass the biased potential. We can see that in PP the spin have both positive and negative values in the system, leading to the zero average magnetization, while in FP the spin is prone to be down so that the system can be averagely magnetized.

Finally, we consider the effects of temperature on the relevant physical result. The factor of temperature can be introduced by the Fermi-Dirac distribution function $f_\beta(\varepsilon) = \frac{1}{\exp[\beta(\varepsilon-\varepsilon_F)]+1}$, where $\beta = k_B T$, $k_B$ is the Boltzmann factor and $T$ is the temperature. When at a finite temperature, the probability of the fermion occupying one specific energy state can be described by $f_\beta(\varepsilon)$. In Figure 5 we plot the dependence of average magnetization on interaction strength $U$ for systems with disorder strengths $g = 1$ and $g = 2$ at different temperatures $T$ which are also scaled with energy units $t$. The doping density is assumed to be $\delta n = 1\%$ as before. We can see that at realistic finite temperatures ($T = 0.05$) the average

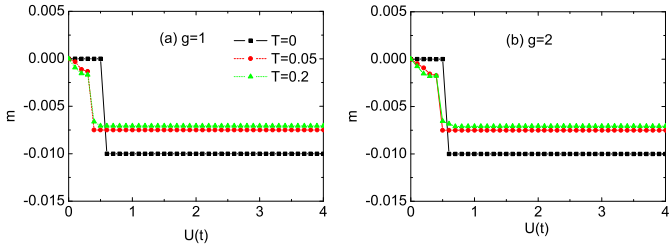


**Fig. 5.** (Color online) The average magnetization $m$ versus the interaction strength $U$ at finite temperature $T$ with disorder strength (a) $g = 1$ and (b) $g = 2$. Symbols for different temperatures are indicated in (a). Doping density $\delta n = 1\%$.

magnetization can also reach the saturation value and the nature of the PFPT first-order transition is not changed, but the saturate value of $m$ is smaller than that in the case of zero temperature. With the increase of temperature the saturation value decreases for all investigated values of $g$ and $U$. All the values of $m$ are smaller than 0.01 which is the maximum value corresponding to the full polarization of the doping electrons. This indicates that at finite $T$ the doping electrons are only partially polarized due to the effect of thermal fluctuations. Also we can see that at finite temperature, the critical value of $U_c$ is a little larger at $g = 2$ than $g = 1$, which is consistent with the previous conclusion.

## 4 Discussions and summaries

It is well known that a single layer graphene is unstable against the antiferromagnetic correlation [27] in the presence of defects. In our calculations, we find that there is no AF order in the ground state in all the cases under consideration, but only the paramagnetic phase and ferromagnetic phase exists, which denotes that the above two kinds orders are energy favored.

In conclusion, by using the mean-field approach to deal with the Hubbard interaction, we numerically calculate the effect of the site-energy disorder on the magnetization of bilayer graphene when the system is low-doped compared with the half-filling. The results show that the site-energy disorder preserves the nature of the first-order PFPT phase transition, but it may enhance the critical interaction strength $U_c$. We give a simple explanation to this conclusion due to the competition between localization caused by disorder and Hubbard interaction. The thermal fluctuations at realistic finite temperature also do not change the behavior of the first-order transition but can decrease the saturate magnetization in FP phase.

We appreciate it a lot for the referees as they gave us so many valuable suggestions. This work was supported by the State Key Programs for Basic Research of China (Grant Nos. 2005CB623605 and 2006CB921803), and by National Foundation of Natural Science in China Grant Nos. 10874071 and 60676056.

## References


1. K.S. Novoselov, A.K. Geim, S.V. Morozov, D. Jiang, Y. Zhang, S.V. Dubonos, I.V. Grigorieva, A.A. Firsov, Science **306**, 666 (2004)
2. C.K. Kane, Nature (London) **438**, 168 (2005)
3. K.S. Novoselov, E. MaCann, S.V. Morozov, V.I. Fal'ko, M.I. Katsnelson, U. Zeitler, D. Jiang, F. Schedin, A.K. Gein, Nat. Phys. **2**, 177 (2006)
4. A.H.C. Neto, F. Guinea, N.M. Peres, K.S. Novoselov, A.K. Geim, Rev. Mod. Phys. **81**, 109 (2009)
5. K.S. Novoselov, A.K. Geim, S.V. Morozov, D. Jiang, M.I. Katnelson, I.V. Grigorieva, S.V. Dubonos, A.A. Firsov, Nature (London) **438**, 197 (2005)
6. Y. Zhang, Y.-W. Tan, H.L. Stormer, P. Kim, Nature (London) **438**, 201 (2005)
7. C.-H. Zhang, Y.N. Joglekar, Phys. Rev. B **77**, 233405 (2008)
8. S.-J. Xiong, Y. Xiong, Phys. Rev. B **76**, 214204 (2007)
9. L. Schweitzer, P. Markos, Phys. Rev. B **78**, 205419 (2008)
10. Y.-X. Wang, S.-J. Xiong, Eur. Phys. J. B **67**, 63 (2009)
11. Y.-Y. Zhang, J. Hu, B.A. Bernevig, X.R. Wang, X.C. Xie, W.M. Liu, Phys. Rev. Lett. **102**, 106401 (2009)
12. K. Ziegler, Phys. Rev. Lett. **102**, 120802 (2009)
13. J. Nilsson, A.H. Castro Neto, N.M.R. Peres, F. Guinea, Phys. Rev. B **73**, 214418 (2006)
14. T. Stauber, N.M.R. Peres, F. Guinea, A.H.C. Neto, Phys. Rev. B **75**, 115425 (2007)
15. H. Min, R. Bistritzer, J.-J. Su, A.H. MacDonald, Phys. Rev. B **78**, 121401(R) (2008)
16. M.Y. Kharitonov, K.B. Efetov, Phys. Rev. B **78**, 241401(R) (2008)
17. R. Bistriter, A.H. MacDonald, Phys. Rev. Lett. **101**, 256406 (2008)
18. E.V. Castro, N.M.R. Peres, T. Stauber, N.A.P. Silva, Phys. Rev. Lett. **100**, 186803 (2008)
19. T. Ohta, A. Bostwick, T. Seyller, K. Horn, E. Rotenberg, Science **313**, 951 (2006)
20. J.B. Oostinga, H.B. Heersche, X. Liu, A.F. Morpurgo, L.M.K. Vandersypen, Nature Mater. **7**, 151 (2008)
21. E. McCann, V.I. Fal'ko, Phys. Rev. Lett. **96**, 086805 (2006)
22. J.-C. Charlier, X. Gonze, J.-P. Michenaud, Phys. Rev. B **43**, 4579 (1991)
23. A. Misu, E. Mendez, M.S. Dresslhaus, J. Phys. Soc. Jpn **47**, 199 (1979)
24. P.W. Anderson, Phys. Rev. **109**, 1492 (1958)
25. J. Fernandez-Rossier, J.J. Palacios, Phys. Rev. Lett. **99**, 177204 (2007)
26. E.H. Lieb, Phys. Rev. Lett. **62**, 1201 (1989)
27. J.J. Palacios, J. Fernandez-Rossier, L. Brey, Phys. Rev. Lett. **77**, 195428 (2008)